**Geomechanics and Engineering**, *Vol. 17, No. 6 (2019) 507-513*
DOI: https://doi.org/10.12989/gae.2019.17.6.507


# Stress-strain behaviour of reinforced dredged sediment and expanded polystyrenes mixture under cyclic loading

Yundong Zhou[1a], Mingdong Li[*2], Kejun Wen[3b] and Ruiming Tong[1c]

[1]*Key Laboratory of Ministry of Education for Geomechanics and Embankment Engineering, Hohai University, Nanjing 210098, China*
[2]*School of Civil Engineering and Architecture, East China University of Technology, Nanchang, 330013, China*
[3]*Department of Civil and Environmental Engineering, Jackson State University, Jackson, MS, 39217, U.S.A.*

*(Received August 1, 2018, Revised February 25, 2019, Accepted March 5, 2019)*

**Abstract.** Reinforced soil and Expanded Polystyrenes (EPS) mixture (RSEM) is a geomaterial which has many merits, such as light weight, wide strength range, easy for construction, and economic feasibility. It has been widely applied to improve soft ground, solve bridge head jump, fill cavity in pipeline and widen highway. Reutilizing dredged sediment to produce RSEM as earthfill can not only consume a large amount of waste sediment but also significantly reduce the construction cost. Therefore, there is an urgent need understand the basic stress-strain characteristics of reinforced dredged sediment-EPS mixture (RDSEM). A series of cyclic triaxial tests were then carried out on the RDSEM and control clay. The effects of cement content, EPS beads content and confining pressure on the cyclic stress-strain behaviour of RDSEM were analyzed. It is found that the three stages of dynamic stress-strain relationship of ordinary soil, vibration compaction stage, vibration shear stage and vibration failure stage are also applicative for RDSEM. The cyclic stress-strain curves of RDSEM are lower than that of control clay in the vibration compaction stage because of its high moisture content. The slopes of backbone curves of RDSEMs in the vibration shear stage are larger than that of control clay, indicating that the existence of EPS beads provides plastic resistance. With the increase of cement content, the cyclic stress-strain relationship tends to be steeper. Increasing cement content and confining pressure could improve the cyclic strength and cyclic stiffness of RDSEM.

**Keywords:** cyclic; stress; strain; constitution; sediment

## 1. Introduction

In coastal area, accumulations of marine sediments can clog waterways and damage coastal breeding basins (Li *et al.* 2017a). Land reclamation is an effective way to reutilize the dredged sediment and/ or to overcome the shortage of land (Bo *et al.* 2015, Chris *et al.* 2018, Dhritiraj *et al.* 2015). Because of the poor properties, such as high compressibility, low strength and low permeability, the reclaimed sediment is a challenge of public infrastructure development, such as highway, railway and city subway (Cai *et al.* 2017, Wang *et al.* 2016, 2017). Many difficulties had been confronted, including the bumping at bridge-head and settlement of soft foundation (Li *et al.* 2017b).

Reinforced soil-Expanded Polystyrenes (EPS) mixture is a type of artificial material that consists of soil, EPS beads and binding agent. Cement mixed with fly ash, lime and waste gypsum were normally adopted as binding agent to improve the mechanical performance. Household waste foam plastic could be used to save cost (Liu 2013). The best grain size of EPS beads is 3-5 mm in construction (Hou 2012). Waste soils generated from engineering constructions can be reused as ingredient of Reinforced soil-EPS mixture (RSEM) (Li *et al.* 2017b).

RSEM has many merits, such as the light weight, adjustability of strength, and fluidity. It had been applied in many engineering practices since 1980s, including the treatments of soft foundation, bumping at bridge head, backfill of pipelines and widening of highway, etc., as shown in Fig. 1 (Nagase *et al.* 2000, Li *et al.* 2006). Reutilizing dredged sediment to produce RSEM as earth fill can not only consume a large amount of waste sediment, but also reduces the cost significant

There are many research achievements on RSEM. A model for compaction density of RSEM was established, based on the material proportion and physical essence of soil compaction (Hou 2014). It was verified by lab tests that the predicted value was close to the measured wet density with relative error between 0.28% and 5.27%, under different compaction levels (Hou 2014). In addition, it was found that the dry density of RSEM decreased dramatically with the increase of EPS beads content. An increase of 0.1% of EPS beads content resulted in a reduction of the density of RSEM for 10% (Jamshidi Chenari *et al.* 2018). Unconfined compressive strength increased parabolically with the increase of cement content, while decreased hyperbolically with the increase of EPS beads content.

*Corresponding author, Professor
E-mail: ytlimd@163.com
[a]Ph.D.
E-mail: ydzhou@hhu.edu.cn
[b]Ph.D.
E-mail: kejun.wen@jsums.edu
[c]M.Sc.
E-mail: 26304148@qq.com


http://www.techno-press.org/?journal=gae&subpage=7 ISSN: 2005-307X (Print), 2092-6219 (Online)

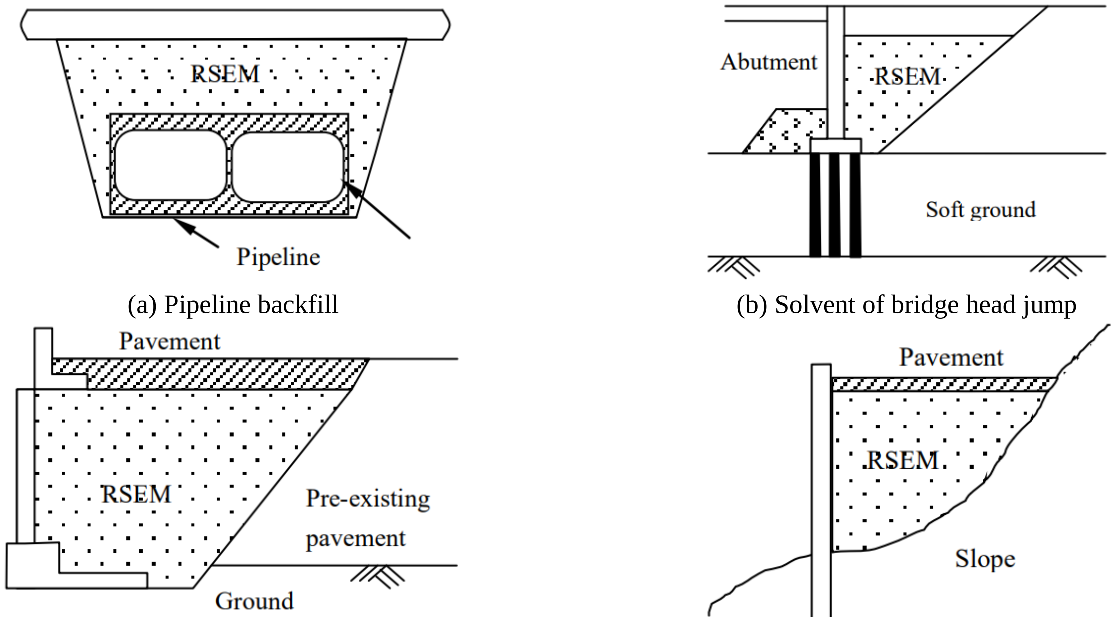


(a) Pipeline backfill (b) Solvent of bridge head jump (c) Road widening (d) Slope earthfill

Fig. 1 The engineering applications of RSEM

Cohesion increased with the increase of cement content because it was mainly caused by the bonding function of hydration products of cement. Friction angle decreased with the increase of EPS beads content, which was caused by the weakening of interaction between EPS beads and sand grains (Karimpour Fard *et al.* 2015). Jamshidi Chenari *et al.* (2016) evaluated the applicability of EPS beads mixed with sand in five different contents and measured some of their fundamental properties. Quantitative relationships between physico-mechanical properties of RSEM and material constituents were provided by Li *et al.* (2017b). Cohesion decreased with the increase of the particle size of EPS beads. The apparent adhesion of the interface was shown to increase with EPS content, while the friction angle of the interface was shown to decrease with EPS content (Alaie *et al.*, 2018).

The properties of soil under cyclic loading have been a research focus in geomechanics (Hsiao *et al.* 2016, Im *et al.* 2017, Huang *et al.* 2017, Tafreshi *et al.* 2018). As for the properties of RSEM under dynamic loads or cyclic loads, Bathurst *et al.* (2007) found that the damage caused by dynamic loading could be effectively reduced by RSEM. Data from stress-controlled cyclic uniaxial tests showed a logarithmic decrease in the damping ratio of EPS geofoam with the increasing axial strain amplitude. EPS beads content was reported to have a slight influence on the initial shear modulus of RSEM as well as the cyclic stress-strain curve in the linear elastic stage. However, the increasing EPS beads content obviously reduced the dynamic strength. It was found that the initial shear modulus increased with the increasing initial minor principal stress for the isotropically and anisotropically consolidated specimens (Gao *et al.*, 2015, 2017). The cyclic deformation mode of RSEM was different from that of fine sand. RSEM should be considered as viscous elastic material instead of elastic material (Gao *et al.* 2017). The shear stress attenuated more rapidly with depth in RSEM than that in fine sand (Cai *et al.* 2016). For cyclic axial strain amplitude greater than 1.0%, RSEM exhibited a visco-elasto-plastic behavior associated with the occurrence of permanent plastic strains at the end of the cyclic tests (Trandafir *et al.* 2010).

It can be found that the properties of RSEM under static and dynamic loading have been a hot research topic in geomechanics. However, there is little research on RDSEM, where the soil is very soft and fully saturated. The goal of this study is to investigate the stress-strain behaviour of RDSEM under cyclic loading, one of the fundamental dynamic properties, which are essential to determine the deformation and stability of earth fill under cyclic loads. Dynamic triaxial tests on RDSEM with different constituents and control clay were carried out in laboratory. Stress-strain relationships of RDSEM were obtained, analyzed and compared with that of control clay. The effects of cement content, EPS beads content and confining pressure were presented and discussed.

## 2. Materials and methods

### *2.1 Dredged sediment and control clay*

The dredged sediment adopted in this study is a kind of marine sediment, collected from Lianyungang, China. The control clay was collected from 6 meters below the ground surface of the Olympic Sports Center, located in Hexi, Nanjing, China. Geotechnical properties and mineral compositions of them are shown in Tables 1 and 2 respectively, while the particle distribution curves are shown in Fig 2

### *2.2 Cement*

The cement used in this study was #32.5 Portland

Table 1 Geotechnical properties of the material dredged sediment and control clay

| Soil | Unit Weight $\gamma$ ($kN \cdot m^{-3}$) | Moisture Content $\omega$(%) | Void Ratio $e$ | Specific Gravity $Gs$ | Plastic Limit $\omega_P$(%) | Liquid Limit $\omega_L$(%) |
|---|---|---|---|---|---|---|
| Dredged sediment | 14.5 | 63.8 | 1.98 | 2.72 | 27.5 | 51.3 |
| Control clay | 16.4 | 32.5 | 1.68 | 2.73 | 27.3 | 47.5 |

Table 2 Mineral compositions of the material dredged sediment and control clay

| Minerals | $SiO_2$ | $Al_2O_3$ | $Fe_2O_3$ | CaO | MgO | $K_2O$ | $Na_2O$ | $SO_3$ | Cl | LOI |
|---|---|---|---|---|---|---|---|---|---|---|
| Dredged sediment | 50.45 | 15.94 | 6.13 | 5.25 | 2.52 | 3.33 | 1.68 | 0.24 | 0.69 | 6.50 |
| Control clay | 51.98 | 18.35 | 8.33 | 2.49 | 2.31 | 3.54 | 0.77 | 0.09 | 0.02 | 8.80 |

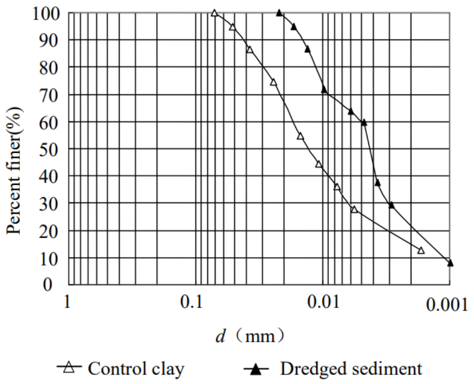


Fig. 2 Particle size distribution curves of different materials

cement, procured from Zhongshan Cement Factory Co. LTD, Nanjing, China.

### *2.3 EPS beads*

EPS is a macromolecule polymer with prior lightweight properties, where large number of closed bubbles were formed during the process of foaming. The EPS beads adopted in this study were procured from Nanjing Youbang Foamed Plastic Co. LTD, with density of 0.023 g/cm$^3$ and average diameter of 3 mm.

### *2.4 Test combinations of RDSEM*

Table 3 illustrates different test combinations of RDSEM. The value of $\alpha$ indicates cement content by weight of the dry sediment, while $\beta$ denotes EPS beads content by weight of the dry sediment.

### *2.5 Preparation of specimens*

The required materials were prepared, portioned and weighed. They were mixed thoroughly using blender at 100 RPM. The RDSEM mixtures were then put into mold with an inner diameter of 5 cm in and height of 12 cm. They were vibratory compacted to assume the skeletal relative density. The RDSEM specimens were cured in an oven at 20 ± 2℃ and 99% humidity for 72 hours in the mold. They were then taken out of the mold and put into the oven to

Table 3 The test combinations of cement content and EPS beads content

| Test No. | $\alpha$ (%) | $\beta$ (%) |
|---|---|---|
| T11 | 5 | 2 |
| T12 | 5 | 3 |
| T13 | 5 | 4 |
| T21 | 10 | 2 |
| T22 | 10 | 3 |
| T23 | 10 | 4 |
| T31 | 15 | 2 |
| T32 | 15 | 3 |
| T33 | 15 | 4 |
| CC | 0 | 0 |

*CC is control clay

cure for additional 23 days. Four specimens were prepared for each test specification. The cross-sections of T11, T12 and T13 are shown in Fig. 3. The specimens were placed in air ventilator and vacuumed for 20 mins at a vacuum degree of -0.1 MPa. Finally, the specimens were fully saturated through opening the water inlet valve. The saturated specimens remained in aqueous environment for another 24 hours.

### *2.6 Measurement methods*

The specimens were tested by cyclic triaxial apparatus which was designed and fabricated by Hohai University and Japan Round Well Co., LTD. Specimens were placed in triaxial cell connected with vibration equipment. A cell pressure (20 kPa) was applied to saturate the pipe line around 30 mins until there is no air bubble in the drainage lines. A back pressure (100 kPa) was then applied to the specimen to saturate it completely. Certain confining pressures (30 kPa, 60 kPa and 90 kPa) were applied to the specimens for consolidation. The consolidation process was finished, when the volume change of the specimen reached less than 0.1 mL in 5 mins. After consolidation, undrained cyclic shear tests were conducted. The cyclic loads applied were in the form of sine wave with a frequency of 0.1 Hz. The amplitude is controlled by the cyclic shear stress ratio (CSSR), as shown in Eq. (1). The cyclic axial loads were applied by stages and each stage corresponding to a given CSSR. The magnitude of the CSSR for the first stage was 0.05, and it increased to 0.1 in the second stage, after that the CSSR was increased by 0.1 at each stage. For each stage, 10 cycles of shear stress were performed under stress-controlled condition. The tests were stopped until axial strain exceeded 5%. The test parameters are listed in Table 4.

$$CSSR = \frac{\tau_d}{\sigma_c} = \frac{\sigma_d}{2\sigma_c} \tag{1}$$

where $\tau_d$ is the cyclic shear stress amplitude in 45° plane, $\sigma_c$ is the consolidation confining pressure, and $\sigma_d$ is amplitude of axial cyclic load.

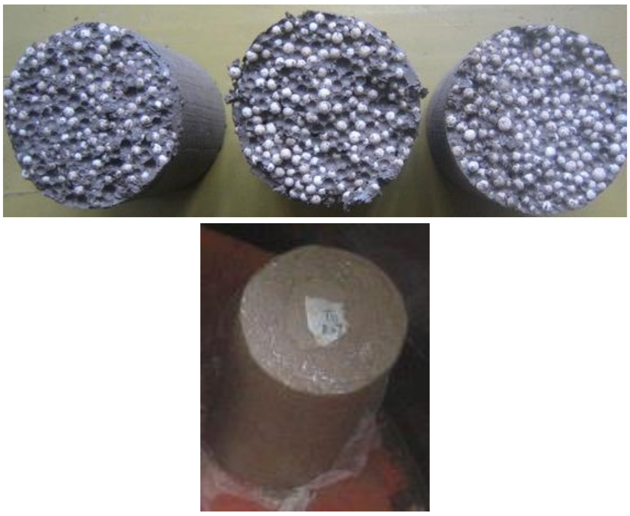

Fig. 3 Cross sections of the T11, T12, T13 specimens and control clay specimen

Table 4 Cyclic shear test parameters

| Confining pressures | CSSR | Cyclic load frequency | Cycles |
|---|---|---|---|
| 30 kPa, 60 kPa, 90 kPa | 0.05, 0.1, 0.2, 0.3, 0.4, 0.5… (until axial strain reached 5%) | 0.1 Hz | 10 |

## 3. Results and discussions

The relationship between the maximum cyclic axial deviatoric stress and the maximum cyclic axial strain at different CSSRs is named as the backbone curve, which represents the dynamic stress-strain relationship of soils (Das and Luo 2017). Characteristics and rules of backbone curves of RDSEM are presented and discussed subsequently.

### *3.1 Characteristics of cyclic stress-strain relationship of RDSEM*

The backbone curves of RDSEM and control clay are shown in Fig. 4. The axial strain increases with the increase of cyclic axial stress, but the slopes of backbone curves decrease with the increasing strain. In the end, some stress-strain relationships level off. With the increase of load cycles, the deformation of RDSEM can be classified into three stages, i.e., vibration compaction stage, vibration shear stage and vibration failure stage. At the initial stage, the stress level is low and the deformation of the RDSEM is small. In addition, the stress-strain curve exhibits as linearity. The deformation of soil was mainly demonstrated as vibration compaction deformation caused by the vertical displacement of soil particles. The soil structure was not destroyed. This is identified as the vibration compaction stage. After that, with the progress of the load cycles, the stress level rises up gradually and larger deformation occurs. The stress-strain relationship is found to be no longer in a linear relationship, where plastic deformation takes place. This represents the vibration shear stage. With further increase of the load cycles, the stress level remains constant or rose up rarely, but the deformation increases gradually, indicating the gradual damage of soil structure.

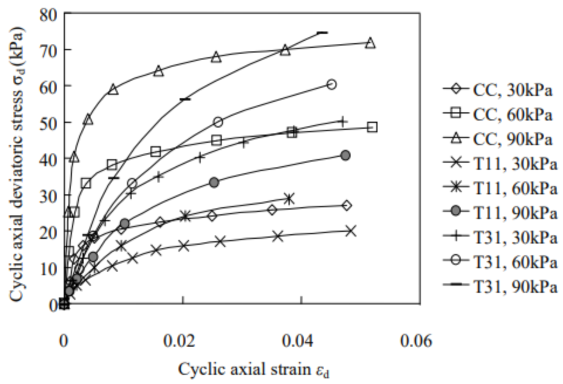


Fig. 4 The backbone curves of RDSEM and CC

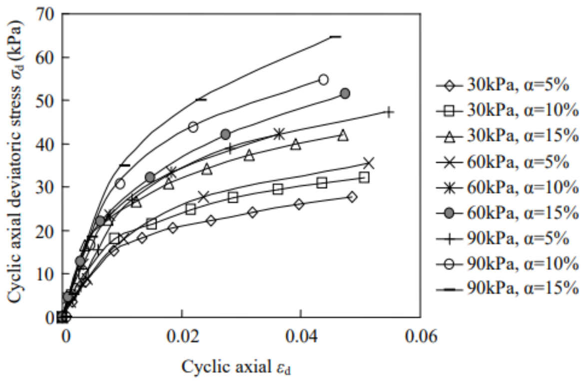


Fig. 5 The backbone curve of RDSEM with different cement contents (EPS beads content 3%)

When the strain reaches 5%, the soil structure can be recognized as broken. The last process is the vibration failure stage. Take T11 under the confining pressure of 30 kPa as an example, vibration compaction stage covers the strain scope of 0-0.002, vibration shear stage covers the strain scope of 0.002-0.027, and vibration failure stage covers strain larger than 0.027. In the vibration compaction stage, the slopes of the backbone curves of RDSEM are obviously lower than that of the control clay. It indicates RDSEMs are softer than control clay because of higher moisture contents. This is consistent with the result s of Yan *et al.* (2018). During the vibration shear stage, the slopes of backbone curves of RDSEMs are larger than that of control clay, and much better than PM4Silt (a kind of silt studied by Ross *et al.* (2018)) whose cyclic stress decreased with the load cycles after 3 cycles (Ross *et al.* 2018). This means that the existence of EPS beads provides plastic resistance.

### *3.2 Effect of cement content on cyclic stress-strain relationship of RDSEM*

It was reported that cement content increased the slope of stress-strain curves both before and after reaching the peak compressive stress value under static loads (Jamshidi Chenariet *et al.* 2018). Fig. 5 shows the effect of cement content on the backbone curve of RDSEMs under cyclic loads. Under the same confining pressure, the cyclic stress-strain relationships tend to be steeper with the increasing cement content. This is the same tendency as that under static loads reported by Jamshidi Chenariet *et al.* (2018).

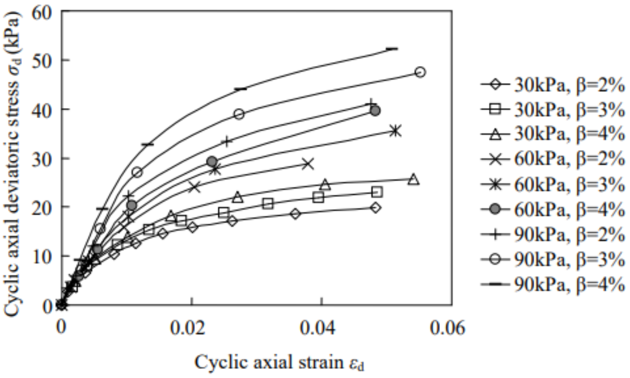


(a) Cement content α=5%

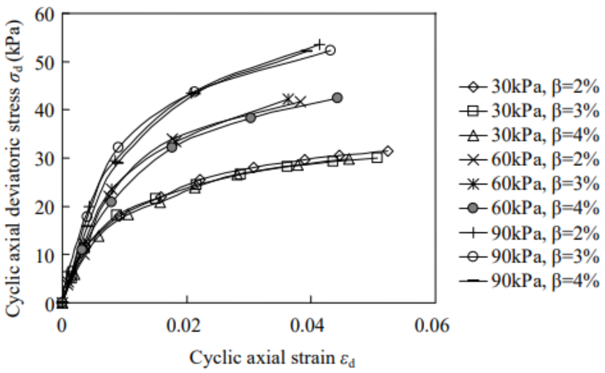


(b) Cement content α=10%

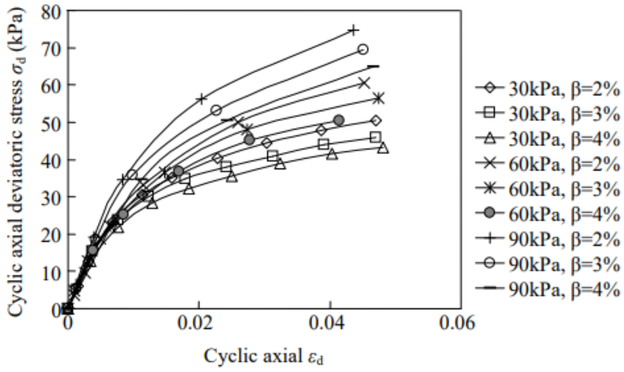


(c) Cement content α=15%

Fig. 6 The backbone curves of RDSEM with different EPS beads contents under different confining pressures

The reason exists in the cementation function of hydration products of cement as well as the porosity reduction function of calcium hydroxide. The reactions were expressed by Eqs. (2) and (3) (Jamshidi Chenariet *et al.* 2018). Fortunately, no sudden failure was observed under cyclic loads when cement content was lower than 15%.

$$6(3CaO.SiO_2)+18H_2O \rightarrow 5CaO.6SiO_2+13Ca(OH) \qquad (2)$$

$$3CaO.Al_2O_3+6H2O \rightarrow 3CaO.Al_2O_3.6H_2O \qquad (3)$$

### *3.3 Effect of EPS beads content on cyclic stress-strain relationship of RDSEM*

The backbone curves of RDSEMs with different EPS beads contents under different confining pressures are shown in Fig. 6. When the cement content is 5% (Fig. 6(a)), the backbone curves of RDSEMs ascend with the increase of EPS beads content, which indicates that the increase of EPS beads content would improve the cyclic modulus and strength of RDSEM when cement content was low. When the cement content is 15% (Fig. 6(c)), the backbone curves of RDSEMs descend with the increase of EPS beads content, which indicates that the increase of EPS beads content could reduce the cyclic modulus and strength of RDSEM when cement content was high. When the cement content is 10% (Fig. 6(b)), the backbone curves of RDSEM with different EPS beads contents overlap with each other and no significant trend of variation happens, which indicates that the increase of EPS beads content had no significant effect on the cyclic stress-strain relationship of RDSEM with this cement content. To interpret this phenomenon, shear strengths of EPS beads and cement stabilized dredged sediment under the confining pressure of 60 kPa were tested, as shown in Fig. 7. The shear strength of cement stabilized dredged sediment increases with the increasing cement content. When cement content is 5%, the strength of cement stabilized soil is lower than that of EPS beads. When cement content is 10%, cement stabilized soil presents similar strength to that of EPS beads. When cement content is 15%, cement stabilized soil achieves much higher strength than that of EPS beads. Additionally, increasing cement content increases the hardness and reduces the compressibility of RSEM (Jamshidi Chenariet *et al.* 2018). As a conclusion, the effect of EPS beads content on the

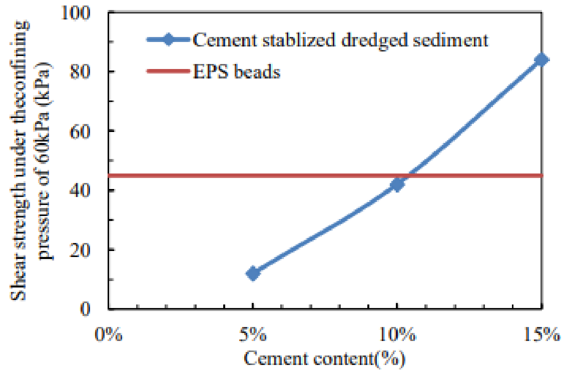


Fig. 7 Shear strength of cement stabilized dredged sediment and EPS beads

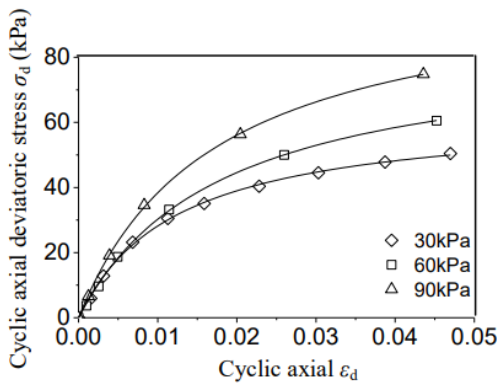


Fig. 8 The backbone curve of RDSEM (T31) under different confining pressures

cyclic stress-strain relationship relies on the relative strength and stiffness of the EPS beads to cement stabilized dredged sediment. When the strength and stiffness of EPS beads are higher than that of cement stabilized dredged sediment, the backbone curves of RDSEMs ascend with the increase of EPS beads content, vice versa. When the strength and stiffness of EPS beads are similar to that of cement stabilized soil, EPS beads content has little influence on the backbone curves of RDSEMs.

### *3.4 Effect of confining pressure on cyclic stress-strain relationship of RDSEM*

The backbone curves of RDSEM (T31) at different confining pressures are shown in Fig. 8. The cyclic stress-strain relationship of RDSEM tends to increase with the increasing confining pressure, indicating that the increase of confining pressure could increase the strength and rigidity of RDSEM. This is consistent with other studies on RSEMs and ordinary soil (Gao *et al.* 2015, Ross *et al.* 2018).

## 4. Conclusions

A series of cyclic triaxial tests were conducted on RDSEMs to study their stress-strain behaviour under cyclic loads. The characteristics of backbone curves of RDSEM were analyzed and compared with control clay. Effects of cement content, EPS beads content and confining pressure on the cyclic stress-strain relationship were presented and discussed. The following conclusions can be made.

• The three stages of dynamic stress-strain relationship of ordinary soil, i.e., vibration compaction stage, the vibration shear stage and the vibration failure stage, were also applicative for RDSEM.

• Because of the high moisture content, RDSEMs were softer than control clay, resulting in the lower cyclic stress-strain curves of RDSEM in the vibration compaction stage.

• During the vibration shear stage, the slopes of backbone curves of RDSEMs were larger than that of control clay, indicating that the existence of EPS beads provided plastic resistance.

• With the increase of cement content, the cyclic stress-strain relationship tended to be steeper. The reasons existed in the cementation function and porosity reduction function of hydration products of cement. Increasing the cement content and confining pressure could improve the cyclic strength and cyclic stiffness of RDSEM.

• The effect of EPS beads content on the cyclic stress-strain relationship relied on the relative strength and stiffness of the EPS beads to cement stabilized dredged sediment. When the strength and stiffness of EPS beads are higher than that of cement stabilized soil, the backbone curves of RDSEMs ascended with the increase of EPS beads content. In contrast, they descended. When the strength and stiffness of EPS beads were similar to that of cement stabilized soil, EPS beads content had little influence on the backbone curves of RDSEMs.

## Acknowledgements

This study is supported by the National Foundation of China under Grant No. 51869001 and 51609093, Jiangsu Planned Projects for Postdoctoral Research Funds under Grant No. 1601007A, and a grant from Jiangsu Power Design Consulting Co., Ltd. The assistance from Yifei Sun and Ubani Ogbonnaya in improving the English writing is greatly appreciated.

## References

Alaie, R. and Jamshidi Chenari, R. (2018), "Cyclic and post-cyclic shear behaviour of interface between geogrid and EPS beads-sand backfill", *KSCE J. Civ. Eng.*, **22**(9), 3340-3357.

Bathurst, R.J., Zarnani, S. and Gaskinc, A. (2007), "Shaking table testing of geofoam seismic buffers", *Soil Dyn. Earthq. Eng.*, **27**(4), 324-332.

Bo, M.W., Arulrajah, A., Horpibulsuk, S., Chinkulkijniwat, A. and Leong, M. (2016), "Laboratory measurements of factors affecting discharge capacity of prefabricated vertical drain materials", *Soil. Found.*, **56**(1), 129-137.

Cai, X., Gao, H., Zhao, H., Chen, G. and Chen, R. (2015), "Dynamic characteristics of EPS beads composite lightweight soil under railway loading", *J. Disaster Prevent. Mitig. Eng.*, **35**(5), 651-658.

Cai, Y., Qiao, H., Wang, J., Geng, X., Wang, P. and Cai, Y. (2017), "Experimental tests on effect of deformed prefabricated vertical drains in dredged soil on consolidation via vacuum preloading", *Eng. Geol.*, **222**, 10-19.

Das, B.M. and Luo, Z. (2017), *Principles of Soil Dynamics*, Cengage Learning, U.S.A.

Dhritiraj, S., Ruishan, C. and Michael, E.M. (2018), "Building beyond land: An overview of coastal land reclamation in 16 global megacities", *Appl. Geograph.*, **90**, 229-238.

Gao, H., Chen, R., Tong, F., Chen, G. and Cai, X. (2015), "Dynamic modulus and damping ratio of EPS bead composite soil under complex stress conditions", *J. Disaster Prevent. Mitig. Eng.*, **35**(2), 166-172, 198.

Gao, H., Hu, Y., Wang, Z., Wang, C. and Chen, G. (2017), "Shaking table tests on the seismic performance of a flexible wall retaining EPS composite soil", *Bull. Earthq. Eng.*, **15**(12), 5481-5510.

Hou, T. (2012), "Influence of expanded polystyrene size on deformation characteristics of light weight soil", *Cent. South Univ.*, **19**(11), 3320-3328.

Hou, T. (2014), "Model for compaction density and engineering properties of light weight soil", *Chin. J. Geotech. Eng.*, **36**(11), 2127-2135 (in Chinese).

Hsiao, D., Phan, V.T. and Huang, C. (2016), "An experimental investigation on dynamic properties of various grouted sands", *Geomech. Eng.*, **10**(1), 77-94.

Huang, M., Xu, C., Zhan, J. and Wang, J. (2017), "Comparative study on dynamic properties of argillaceous siltstone and its grouting-reinforced body", *Geomech. Eng.*, **13**(2),333-352.

Im, J., Tran, A., Chang, I. and Cho, G. (2017), "Dynamic properties of gel-type biopolymer-treated sands evaluated by Resonant Column (RC) Tests", *Geomech. Eng.*, **12**(5), 815-830.

Jamshidi Chenari, R., Fatahi, B., Ghorbani, A. and Nasiri Alamoti, M. (2018), "Evaluation of strength properties of cement stabilized sand mixed with EPS beads and fly ash", *Geomech. Eng.*, **14**(6), 533-544.

Jamshidi Chenari, R., Mehran Karimpour, F., Pourghaffar Maghfarati, S., Pishgar, F. and Lemos Machado, S. (2016), "An investigation on the geotechnical properties of sand–EPS mixture using large oedometer apparatus", *Construct. Build. Mater.*, **113**(15), 773-782.

Karimpour Fard, M., Jamshid Chenari, R. and Soheili, F. (2015), "Shear strength characteristics of sand mixed with EPS beads

using large direct shear apparatus", *Elec*. *J*. *Geotech*. *Eng*., **20**(8), 2205-2220.
Li, M., Cong, X., Zhu, L., Kong, L., Zhang, Z., Tian, A. and Li, L. (2017a), "Experimental study on recycling dredged marine sediment and phosphate tailing to produce earth fill", *Mar*. *Georesour*. *Geotechnol*., **35**(4), 586-591.
Li, M., Wen, K., Li, L. and Tian, A. (2017b), "Mechanical properties of expanded polystyrene beads stabilized lightweight soil", *Geomech*. *Eng*., **13**(3), 459-474.
Li, M., Zhu, W., Ma, D. and Ji, F. (2006), "Construction technology and application in-situ of expanded polystyrene treated lightweight soil", *Chin*. *J*. *Geotech*. *Eng*., **28**(4), 533-536 (in Chinese).
Liu, H. (2013), "Technological innovation methods and practices in geotechnical engineering", *Chin*. *J*. *Geotech*. *Eng*., **35**(1), 34-58 (in Chinese).
Marshall, C., Large, D.J., Athab, A., Evers, S.L., Sowter, A., Marsh, S. and Sjögersten, S. (2018), "Monitoring tropical peat related settlement using ISBAS In SAR, Kuala Lumpur International Airport (KLIA)", *Eng*. *Geol*., **244**(3), 57-65.
Nagase, K. and Kobayashi, H. (2000), "Development of a lightweight soil with Styrofoam", *Soil*. *Found*., **48**(6), 13-15.
Ross, W.B., Adam, B.P. and Katerina, Z. (2018), "Constitutive modeling of the cyclic loading response of low plasticity fine-grained soils", *Proceedings of the GeoShanghai 2018 International Conference: Fundamentals of Soil Behaviors*, Shanghai, China, May.
Tafreshi, S.N.M., Darabi, N.J. and Dawson, A.R. (2018), "Cyclic loading response of footing on multilayered rubber-soil mixtures", *Geomech*. *Eng*., **14**(2), 85-96.
Trandafir, A.C., Bartlett, S.F. and Lingwall, B.N. (2010), "Behavior of EPS geofoam in stress-controlled cyclic uniaxial tests", *Geotext*. *Geomembr*., **28**(6), 514-524.
Wang, J., Cai, Y., Ma, J., Chu, J., Fu, H., Wang, P. and Jin, Y. (2016), "Improved vacuum preloading method for consolidation of dredged clay-slurry fill", *J*. *Geotech*. *Geoenviron*. *Eng*., **142**(11), 06016012.
Wang, J., Ni, J., Cai, Y., Fu, H. and Wang, P. (2017), "Combination of vacuum preloading and lime treatment for improvement of dredged fill", *Eng*. *Geol*., **227**, 149-158.
Yan, C., Xu, X. and Huang, L. (2018), "Identifying the impact factors of the dynamic strength of mudded intercalations during cyclic loading", *Adv*. *Civ*. *Eng*.

*CC*